NUMERICAL INVESTIGATION OF THE TANGENTIAL TWIST OF AN INCOMPRESSIBLE VISCOUS FLUID JET

P. S. Kuts and V. A. Dolgushev

UDC 532.527

The problem of the formation of eddy flow of tangential twist is examined. The fluid flow mode is laminar. The flow parameters are found by the numerical solution of the complete system of Navier–Stokes equations.

Twisted flows in pipes are used extensively in the operation of different kinds of injector and feeder units, refrigerators, a number of separator constructions, highly forced furnace, heater, and drying chambers. In this connection, the hydrodynamics of eddy streams has been the object of careful study for several decades [1, 2]. There are some tens of theoretical papers in which attempts are made to clarify the physical substance of the eddy effect and to construct its mathematical model. The majority of papers are based on the following physical hypotheses:

1) the plane vortex model [3, 4];
2) the hollow twisted jet model [5, 6];
3) the model of free vortex conversion into a forced vortex [7-9].

The hypothesis of the physical origination of an eddy flow in the entrance section of a pipe and its conversion into a forced eddy, which corresponds to the following physical model, underlies the study of the eddy effect in this paper: jet is blown tangentially into a cylindrical chamber, at some distance from the blind end-face wall, which twists the fluid in the chamber.

Such a flow scheme is graphically explicable physically and is strictly described by a system of equations. Assuming the flow to be isothermal at this stage and the fluid properties constant, let us use the axisymmetric system of Navier–Stokes and continuity equations

$$v\frac{\partial v}{\partial r}+u\frac{\partial v}{\partial x}-\frac{w^2}{r}=-\frac{\partial P}{\partial r}+\frac{1}{\mathrm{Re}}\left(\frac{\partial^2 v}{\partial r^2}+\frac{\partial^2 v}{\partial x^2}+\frac{1}{r}\frac{\partial v}{\partial r}-\frac{v}{r^2}\right), \tag{1}$$

$$v\frac{\partial u}{\partial r}+u\frac{\partial u}{\partial x}=-\frac{\partial P}{\partial x}+\frac{1}{\mathrm{Re}}\left(\frac{\partial^2 u}{\partial r^2}+\frac{\partial^2 u}{\partial x^2}+\frac{1}{r}\frac{\partial u}{\partial r}\right), \tag{2}$$

$$v\frac{\partial w}{\partial r}+u\frac{\partial w}{\partial x}+\frac{wv}{r}=\frac{1}{\mathrm{Re}}\left(\frac{\partial^2 w}{\partial r^2}+\frac{\partial^2 w}{\partial x^2}+\frac{1}{r}\frac{\partial w}{\partial r}-\frac{w}{r^2}\right), \tag{3}$$

$$-\frac{\partial}{\partial r}(rv)+\frac{\partial}{\partial x}(ru)=0. \tag{4}$$

Let us seek the solution of the system of equations in a rectangle, one of whose sides lies on the axis of symmetry of the chamber, another is on the generatrix, the third is on the blind end-face wall, and the fourth will be removed to the distance at which the viscous incompressible fluid rotates as a solid (forced eddy) in the numerical experiment [7-9].

Let x and r denote the distances measured, respectively, from the blind end-face wall along the axis of symmetry and from the pipe axis in the radial direction.

A. V. Lykov Institute of Heat and Mass Transfer. Academy of Sciences of the BelorussianSSR. Minsk.
Translated from Inzhenerno-Fizicheskii Zhurnal, Vol. 30, No. 6, pp. 1047-1054, June, 1976. Original article submitted June 30, 1975.

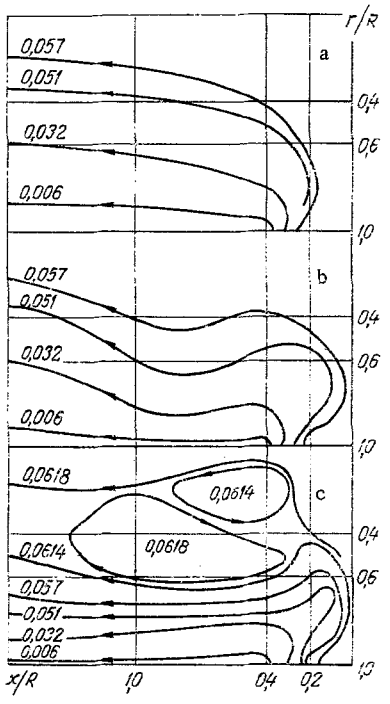

Fig. 1

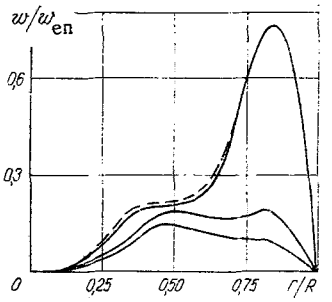

Fig. 2

Fig. 1. Influence of the Reynolds number on the eddy flow configuration. Isostreamlines: a) for Re = 10; b) Re = 1000, c) Re = 66,000.

Fig. 2. Profiles of the tangential component at the sections x = 0.5; 1.0; 1.4, respectively; result obtained on a 63 × 30 mesh for comparison is shown by dashes.

The x, r in the initial system of equations (1)-(4) are normalized with respect to R, v, w, $u-w_{en}$, $P-\rho w_{en}^2$ and the Reynolds number is defined as follows: $Re = w_{en} R/\nu$. Then r and x vary in the domains $0 \leq r \leq 1$, $0 \leq x \leq x_0$, respectively, and the tangential nozzle is located in the subdomain $x_\mu \leq x \leq x_p$. The coordinates of the mesh modes vary within the intervals $1 \leq j \leq JR$, $1 \leq i \leq IX$.

Eddy flow was analyzed in [10, 11] on the basis of the Navier-Stokes equations. Use of such an approach is made difficult, according to the remark in [12], by the lack of knowledge about the boundary conditions needed for uniqueness of the solution.

In our case, the main difficulty is giving the boundary conditions of the tangential input. The possibilities of a tangential supply of fluid in a pipe are quite diverse. The supply may be accomplished by means of one or more holes or around the pipe circumference [2]. The holes may be circular, oval, or rectangular in cross section; hence, a different distribution of the delivered fluid along the perimeter of the pipe cross section and its length, as well as a deviation from the tangential input ($\varphi_{\mu x}, \varphi_{\mu r}$), is possible.

Since the configurations of the tangential nozzle sections and their quantity exert no governing influence on the aerodynamics of the gas streams in an eddy chamber [13], but the flow itself is axisymmetric and is conserved even in the case of one tangential insert [14, 15], let us write the mean velocity distribution on the section of the entrance connection, which is uniform over the chamber generator, as follows:

$$u = \cos \varphi_x, \tag{5}$$

$$v = -\cos \varphi_r, \tag{6}$$

$$w = \varepsilon_w, \tag{7}$$

where φ_x and φ_r are determined as a function of the structure parameters φ_{Tx}, φ_{Tr}, R, a and k_a [16]. As has been mentioned above, conditions for the rotation of a solid are given at the exit. The conditions on the axis of symmetry and on the walls are standard. Therefore, a completely definite model of a tangentially twisted flow bounded by walls is obtained.

For the solution let us convert this problem to stream functions ψ, eddies ω, and twist G by means of the formulas

$$u = \frac{1}{r}\frac{\partial\psi}{\partial r};\quad v = -\frac{1}{r}\frac{\partial\psi}{\partial x},\quad \omega = \frac{1}{r}\left(\frac{\partial u}{\partial r} - \frac{\partial v}{\partial x}\right),\quad G = \frac{w}{r}.$$

After conversion, the system of equations and boundary conditions becomes

$$\frac{\partial^2\psi}{\partial x^2} + \frac{\partial^2\psi}{\partial r^2} = \frac{1}{r}\frac{\partial\psi}{\partial r} + r^2\omega, \tag{8}$$

$$\frac{\partial}{\partial x}\left(\frac{r^3}{\mathrm{Re}}\frac{\partial\omega}{\partial x}\right) + \frac{\partial}{\partial r}\left(\frac{r^3}{\mathrm{Re}}\frac{\partial\omega}{\partial r}\right) = r^2\frac{\partial\psi}{\partial r}\frac{\partial\omega}{\partial x} - r^2\frac{\partial\psi}{\partial x}\frac{\partial\omega}{\partial r} + r^3\frac{\partial(G^2)}{\partial x}, \tag{9}$$

$$\frac{\partial}{\partial x}\left(\frac{r^3}{\mathrm{Re}}\frac{\partial G}{\partial x}\right) + \frac{\partial}{\partial r}\left(\frac{r^3}{\mathrm{Re}}\frac{\partial G}{\partial r}\right) = r^2\frac{\partial\psi}{\partial r}\frac{\partial G}{\partial x} - r^2\frac{\partial\psi}{\partial x}\frac{\partial G}{\partial r} - 2r\frac{\partial\psi}{\partial x}G, \tag{10}$$

at the entrance for $x_\mu \le x \le x_p$

$$\psi(x,\ 1) = \cos\varphi_r(x - x_\mu),\ \omega(x,\ 1) = 0,\ G(x,\ 1) = \varepsilon_w, \tag{11}$$

at the exit for $0 \le r \le 1$

$$\psi(x_0,\ r) = \psi(x_p,\ 1)\,r^2,\ \frac{\partial\omega(x_0,\ r)}{\partial x} = 0,\quad G(x_0,\ r) = G(x_p,\ 1), \tag{12}$$

on the walls for $0 \le x \le x_\mu$

$$\psi(x,\ 1) = \psi(x_\mu,\ 1),$$

for $x_p \le x \le x_0$

$$\psi(x,\ 1) = \psi(x_p,\ 1)$$

and for both intervals

$$\omega_{i,JR} = \frac{3}{\rho r_{JR}(\Delta r_{JR})^2}(\psi_{i,JR} - \psi_{i,JR-1}) - 0{,}5\omega_{i,JR-1},\quad G(x,\ 1) = 0,$$

but for $0 \le r \le 1$

$$\begin{gathered}\psi(0,\ r) = \psi(x_\mu,\ 1),\\ \omega_{1,j} = \frac{3}{\rho r_j(\Delta x_1)^2}(\psi_{1,j} - \psi_{2,j}) - 0{,}5\,\omega_{2,j},\\ G(0,\ r) = 0,\end{gathered} \tag{13}$$

and on the axis of symmetry for $0 \le x \le x_0$

$$\begin{gathered}\psi(x,\ 0) = \psi(x_\mu,\ 1),\\ \omega_{i,1} = \omega_{i,2} + (r_2 - r_1)/(r_3 - r_2)(\omega_{i,2} - \omega_{i,3}),\\ G(x,\ 0) = 0.\end{gathered} \tag{14}$$

The system (8)-(10) was solved numerically with the boundary conditions (11)-(14) by the method of build-up. A homogeneous difference scheme of variable directions with second-order accuracy was selected, which is an extension of the scheme developed in [17] to an irregular pattern. For its construction we start from the general form of the second-order parabolic partial differential equation in two independent variables

$$\gamma(z)\frac{\partial u}{\partial\tau} = Lu + f(z,\ \tau),\quad z(x,\ r), \tag{15}$$

where the functional L has the form $Lu = \sum_{\alpha=1}^{2} L_\alpha u$;

$$L_\alpha u = \frac{\partial}{\partial z_\alpha}\left(\lambda_\alpha(z)\frac{\partial u}{\partial z_\alpha}\right) + \nu_\alpha\frac{\partial u}{\partial z_\alpha};$$

$\gamma(z) \ge c_0 > 0$; $\lambda_\alpha(z) \ge c > 0$; c_0, c are constants. The solution of the equation should satisfy the boundary condition

$$u|_\Gamma = q(z,\ \tau) \tag{16}$$

and the initial condition

$$u(z,\ 0) = u_0(z). \tag{17}$$

On the spatial mesh $D_{i,j}(x_i\{i=1, 2, \ldots, IX\}, r_j\{j=1, 2, \ldots, JR\})$ and in time $D_\tau(\tau^k = k\Delta\tau, \{k=0, 1, \ldots\})$, we approximate the differential problem (15)-(17) by the difference problem

$$\gamma \frac{y^{2k+1} - y^{2k}}{\Delta\tau_{2k+1}} = \Lambda_1 y^{2k+1} + \Lambda_2 y^{2k} + \varphi^{2k+1}, \tag{18}$$

$$\gamma \frac{y^{2k+2} - y^{2k+1}}{\Delta\tau_{2k+2}} = \Lambda_1 y^{2k+1} + \Lambda_2 y^{2k+2} + \varphi^{2k+1}. \tag{19}$$

The initial condition

$$y(z,\ 0) = u_0(z) \tag{20}$$

and difference boundary conditions should be appended to (18)-(19); on the time half-spacing

$$y^{2k+1} = 0{,}5\,(q^{2k} + q^{2k+2}) - \frac{\Delta\tau}{2}\,\Lambda_2\,(q^{2k+2} - q^{2k}) \tag{21}$$

for $i=1$ and $i=IX$, and we have on the main time spacing

$$y^{2k+2} = q^{2k+2} \tag{22}$$

for $j=1$ and $j=JR$.

The notation

$$\gamma = \gamma_{i,j},\ \varphi^{2k+1} = f(z,\ \tau^{2k} + \Delta\tau),$$

$$\Lambda_\alpha y = R_\alpha\,(d_\alpha y_{\bar{x}_\alpha})_{x_\alpha} + \left(\frac{\nu_\alpha + |\nu_\alpha|}{2\lambda_\alpha}\right) d^{(+1\alpha)}\, y_{x_\alpha} + \left(\frac{\nu_\alpha - |\nu_\alpha|}{2\lambda_\alpha}\right) d^{(-1\alpha)}\, y_{\bar{x}_\alpha},$$

where

$$R_{\alpha;\, i_\alpha} = \frac{2\lambda_{\alpha;\, i_\alpha}}{2\lambda_{\alpha;\, i_\alpha} + \bar{h}_\alpha |\nu_{\alpha;\, i_\alpha}|},$$

have been used in (18)-(22); we approximate the second derivatives by a second-order divided difference

$$(d_\alpha y_{\bar{x}_\alpha})_{x_\alpha} = (\lambda_{\alpha;\, i_\alpha + 0.5}\, y_{i_\alpha + 1} - (\lambda_{\alpha;\, i_\alpha + 0{,}5} + \lambda_{\alpha;\, i_\alpha - 0.5})\, y_{i_\alpha} + \lambda_{\alpha;\, i_\alpha - 0.5}\, y_{i_\alpha - 1})/\bar{h}_\alpha^2;$$

$$y_{x_\alpha} = (y_{i_\alpha + 1} - y_{i_\alpha})/h_{\alpha;\, +},\quad y_{\bar{x}_\alpha} = (y_{i_\alpha} - y_{i_\alpha - 1})/h_{\alpha;\, -},$$

$$d^{(+1\alpha)} = \lambda_{\alpha;\, i_\alpha + 0{,}5},\quad d^{(-1\alpha)} = \lambda_{\alpha;\, i_\alpha - 0{,}5}.$$

For simplicity, the time index has been omitted in these notations, since it is fixed for a given direction α.

To solve the system (18)-(22) we used a factorization method. Hence, we reduce the difference equations (18)-(19) to the canonical form for this method:

$$a_{1;\, i_1,\, i_2}\, y^{2k+1}_{i_1 - 1,\, i_2} - c_{1;\, i_1,\, i_2}\, y^{2k+1}_{i_1,\, i_2} + b_{1;\, i_1,\, i_2}\, y^{2k+1}_{i_1 + 1,\, i_2} = -\frac{\gamma_{i_1,\, i_2}}{\Delta\tau_{2k+1}}\, y^{2k}_{i_1,\, i_2} - \Lambda_2 y^{2k}_{i_1,\, i_2} - \varphi^{2k+1}_{i_1,\, i_2},$$

$$a_{2;\, i_1,\, i_2}\, y^{2k+2}_{i_1,\, i_2 - 1} - c_{2;\, i_1,\, i_2}\, y^{2k+2}_{i_1,\, i_2} + b_{2;\, i_1,\, i_2}\, y^{2k+2}_{i_1,\, i_2 + 1} = -\frac{\gamma_{i_1,\, i_2}}{\Delta\tau_{2k+2}} y^{2k+1}_{i_1,\, i_2} - \Lambda_1 y^{2k+1}_{i_1,\, i_2} - \varphi^{2k+1}_{i_1,\, i_2},$$

where

$$a_{\alpha;\, i_\alpha,\, i_\beta} = \left[R_{i_\alpha} \left(\frac{\lambda_{i_\alpha}}{(h_{\alpha;\, -})^2} - \frac{\lambda_{i_\alpha + 0{,}5} - \lambda_{i_\alpha}}{(h_{\alpha;\, -})\,(h_{\alpha;\, +})} \right) - \frac{\nu_{i_\alpha} - |\nu_{i_\alpha}|}{2\,(h_{\alpha;\, -})} \frac{\lambda_{i_\alpha - 0{,}5}}{\bar{\lambda}_{i_\alpha}} \right]_{i_\beta},$$

$$b_{\alpha;\, i_\alpha,\, i_\beta} = \left[R_{i_\alpha} \frac{\lambda_{i_\alpha}}{(h_{\alpha;\, -})\,(h_{\alpha;\, +})} + \frac{\nu_{i_\alpha} + |\nu_{i_\alpha}|}{2\,(h_{\alpha;\, +})} \frac{\lambda_{i_\alpha + 0{,}5}}{\bar{\lambda}_{i_\alpha}} \right]_{i_\beta},$$

$$c_{\alpha;\, i_\alpha,\, i_\beta} = a_{\alpha;\, i_\alpha,\, i_\beta} + b_{\alpha;\, i_\alpha,\, i_\beta} + \frac{\gamma}{\Delta\tau},\quad \alpha,\ \beta = 1,\ 2,\ \alpha \neq \beta.$$

As an initial approximation we take either $\psi_{i,j}=0.0006$, $\omega_{i,j}=G_{i,j}=0.01$, or the solution obtained for any other value of the modal parameter. The solution of the equations in the system (8)-(10) is performed in sequence. After each iteration spacing, the boundary values of the eddy function were reevaluated. Having obtained the solution of the boundary-value problem (8)-(14), we determined the u,v,w velocity distribution by an inverse transformation.

The computations were performed on a 39×18 mesh nonuniform along the x axis. To raise the accuracy, the mesh lines were concentrated in the domain of eddy current formation; 18 of the 39 nodes were in the zone $x_\mu \le x \le x_p$. Comparing the results obtained to the checking values (see Fig. 2) computed on a 63×30 mesh permitted us to see that the accuracy of the solution was sufficiently high. The computation was executed on a "Minsk-32" electronic computer. The solution was considered achieved when the maximum relative change in values of the variables became less than 0.005 between successive iterations and this evolved after 400-800 iterations.

The influence of the Reynolds number, which varied between 1 and 66,000, was estimated in the numerical experiments. Attention is turned to the fact (Fig. 1) that the twisting effect, substantially the centrifugal force, mainly shapes the complex eddy flow configuration, and forces associated with gradients in the tangential component of the velocity produce a positive pressure gradient in the flow direction. The twist stabilized the eddy adjacent to the chamber generator, which always originated at the entrance edge during intensive fluid delivery, while a reverse flow formed at the same time in the central portion.

To clarify the analysis, let us note that an increase in the Reynolds number largely implied an increase in the twist, since w_{en} was expanded in v, w in the ratio 0.3 : 0.7 because of structural peculiarities of the chamber.

We observe no influence of twist in the stream configuration in Fig. 1a; the Reynolds number is just 10, the velocity is negligible, the pressure is constant, and laminar flow fills the whole volume.

As the Reynolds number increases, the tangential component grows and a pressure gradient correspondingly originates, which, in turn, exerts influence on the stream configuration by shifting the flow to the circumference of the chamber. However, viscous friction quenches the twist intensity and the flow gradually returns to the center, tending to fill the whole section (Fig. 1b).

High tangential velocities originated near the generators at a significant intensity of the process (Re = 66,000), and under the influence of viscous friction they gradually damp out resulting in significant pressure gradients which become sufficiently great in order to cease reverse flow along the axis. The picture of fully developed eddy flow is shown in Fig. 1c. Besides, central eddies originate in place of reverse currents in our case, since the boundary conditions at the exit have been formed in such a way that drainage is not allowed. The qualitative picture, obtained theoretically, agrees well with the classical picture developed by experimental investigations, which confirms the correctness of the physical hypothesis underlying the investigations.

Only the tangential velocity component is taken into account in the majority of theoretical researches on eddy flow, and moreover, to simplify the problem the boundary condition at the entrance is considered as a forced eddy entirely filling the whole pipe cross section. Profiles of the tangential velocity component in the entrance section and at some distance away are represented in Fig. 2. The kinetics of the damping of the twist due to viscous friction is seen well.

The profile obtained theoretically differs considerably from the profile compiled by means of the forced eddy law at the center and the free eddy law at the circumference, and approximation by the functions $w/r = \text{const}$ for $0 \le r \le r_B$ and $wr = \text{const}$ for $r_B \le r \le R$ is clearly unsatisfactory, since the curvature for the curves is distinct.

The difference, in principle, between eddy flows after a rotating pipe and tangential swirlers should be mentioned. Rotation of the fluid is built up according to the law of a solid, i.e., a forced eddy, to stabilize the stream in only the first case. In all probability, solutions of many fine problems are contained in the explanation of the crux of this difference, exactly as in the case of the known "teapot effect." The behavior of a teapot depends on whether the fluid rotates together with the vessel or in a fixed vessel, where in the latter case the teapots are collected at the center because of secondary eddies.

In conclusion, let us consider the fact of a different determination of the location of the eddy radius by experimenters, which some determine nearer to the center of the chamber $r_B \approx 0.3R$, and others at the circumference $r_B \approx 0.7R$. The difference can be explained by the presence of two maxima in the tangential component, whose location agrees with the r_B noted by the experimenters.

The circumferential maximum of the tangential component degenerates considerably more intensively than the inner maximum during fluid motion along the chamber under the influence of viscous friction, and a time sets in during continuation of this process when only the inner maximum remains. Hence, the circumferential maximum is much more definite in the tangential entrance section, while the inner maximum is more definite at some distance away. In this connection, experimenters find the maximum depending on the section under consideration.

NOTATION

ρ, fluid density; ν, kinematic viscosity; μ, coefficient of dynamic viscosity; v, w, u radial, tangential, and axial fluid velocity components; P, hydrodynamic pressure; R, chamber radius; a, width of the tangential connector; k_a, number of tangential connectors; w_{en}, mean velocity in the tangential entrance; φ_x, angle between the stream velocity vector and the pipe axis; φ_r, angle between the stream velocity vector and the pipe radius; φ_{Tx}, φ_{Tr}, angle between the direction of the tangential entrance direction and the pipe axis and radius, respectively; u_0, constant determined from the law of fluid mass conservation.

LITERATURE CITED

1. A. P. Merkulov, Eddy Effect and Its Application in Engineering [in Russian], Mashinostroenie, Moscow (1969).
2. V. K. Shchukin, Heat Transfer and Hydrodynamics of Internal Streams in Mass Force Fields [in Russian], Mashinostroenie, Moscow (1970).
3. Yu. A. Ivanov, V. D. Katsnel'son, and V. A. Pavlov, in: Aerodynamics and Heat Transfer in Furnace-Boiler Processes. Collection of Articles [in Russian] (edited by G. F. Knorre), Gostoptekhizdat (1958), p. 101.
4. D. P. Lyakhovskii, in: Aerodynamics and Heat Transfer in Furnace-Boiler Processes. Collection of Articles [in Russian] (edited by G. F. Knorre), Gostoptekhizdat (1958).
5. L. A. Vulis and B. P. Ustimenko, Teploénergetika, No. 9 (1954).
6. A. I. Shtym and P. M. Mikhailov, Izv. Vyssh. Uchebn. Zaved., Énerget., No. 11 (1965).
7. L. A. Vulis and A. A. Kostritsa, Teploénergetika, No. 10 (1962).
8. M. G. Dubinskii, Izv. Akad. Nauk SSSR, Otd. Tekh. Nauk, No. 11 (1955).
9. A. J. Reynolds, Z. Angew. Math. Phys., 12, No. 4 (1961).
10. L. M. Milne-Thomson, Theoretical Hydrodynamics, 5th ed., Macmillan (1968).
11. M. G. Dreissen. "Theory of flow in a cyclone," Rev. Industr. Min., Spec. Vol. Coal Preparation, 449 (1950-1951).
12. S. K. Dunn and C. L. Soo, Trans. ASME, J. Appl. Mech., No. 2 (1973).
13. E. D. Baluev and Yu. V. Troyankin, Teploénergetika, No. 2 (1967).
14. Yu. A. Ivanov, V. D. Katsnel'son, and V. A. Pavlov, in: Aerodynamics and Heat Transfer in Furnace-Boiler Processes. Collection of Articles [in Russian] (edited by G. F. Knorre), Gostoptekhizdat (1958), p. 107.
15. P. M. Mikhailov and É. N. Saburov, Izv. Vyssh. Uchebn. Zaved., Énerget., No. 10 (1966).
16. V. A. Dolgushev and G. S. Kabaldin, Thermophysics and Technology of Thermal Drying Processes [in Russian], Inst. Teplo- i Massoobmena im. A. V. Lykov., Akad. Nauk BelorusSSR, Minsk (1974).
17. F. F. Rimek, Inzh.-Fiz. Zh., 21, No. 5 (1971).